Published in final edited form as:
Hepatology. 2014 January ; 59(1): . doi:10.1002/hep.26662.

MiR-494 Within an Oncogenic MicroRNA Megacluster Regulates G1/S Transition in Liver Tumorigenesis Through Suppression of MCC

Lionel Lim[2,3,1], **Asha Balakrishnan**[3,4,1], **Noelle Huskey**[2,3], **Kirk D. Jones**[5], **Mona Jodari**[2], **Raymond Ng**[6], **Guisheng Song**[6], **Jesse Riordan**[7], **Brittany Anderton**[2,3], **Siu-Tim Cheung**[8], **Holger Willenbring**[6,9], **Adam Dupuy**[7], **Xin Chen**[9,10], **David Brown**[11], **Aaron N. Chang**[12], and **Andrei Goga**[2,3,7,13]

[2]Department of Cell & Tissue Biology, University of California, San Francisco, CA, USA

[3]Department of Medicine, University of California, San Francisco, CA, USA

[4]Department of Gastroenterology, Hepatology and Endocrinology, Hannover Medical School, Germany

[5]Department of Pathology, University of California, San Francisco, California

[6]Eli and Edythe Broad Center of Regeneration Medicine and Stem Cell Research, University of California, San Francisco, California

[7]Anatomy and Cell Biology, University of Iowa, Iowa City, IA

[8]Department of Surgery, The University of Hong Kong

[9]Liver Center, University of California, San Francisco, California

[10]Department of Bioengineering and Therapeutic Sciences, University of California, San Francisco, California

[11]Mirna Therapeutics, Inc. /2150 Woodward #150, Austin, TX 78744

[12]Baylor Institute for Immunology Research, Dallas, TX 75204

Abstract

Hepatocellular carcinoma (HCC) is associated with poor survival for patients and few effective treatment options, raising the need for novel therapeutic strategies. MicroRNAs (miRNAs) play important roles in tumor development and show deregulated patterns of expression in HCC. Because of the liver's unique affinity for small nucleic acids, miRNA based therapy has been proposed in the treatment of liver disease. There is thus an urgent need to identify and characterize aberrantly expressed miRNAs in HCC. In our study, we profiled miRNA expression changes in *de novo* liver tumors driven by MYC and/or RAS, two canonical oncogenes activated in a majority of human HCC. We identified an upregulated miRNA megacluster comprised of 53 miRNAs on mouse chromosome 12qF1 (human homolog 14q32). This miRNA megacluster is upregulated in all three transgenic liver models and in a subset of human HCCs. An unbiased functional analysis of all miRNAs within this cluster was performed.

[13]Correspondence: Andrei Goga, 513 Parnassus Ave HSW 601 San Francisco, CA 94143 Andrei.goga@ucsf.edu.
[1]These authors contributed equally to this work
Contact Information: Andrei Goga, M.D., Ph.D., UCSF, Dept. of Cell & Tissue Biology, 513 Parnassus Ave, Box 0512, San Francisco, CA 94143-0512, Tel: 415-476-4191, andrei.goga@ucsf.edu

Conclusion—We found that miR-494 is overexpressed in human HCC, and aids in transformation by regulating the G1/S cell cycle transition through targeting of the Mutated in Colorectal Cancer (MCC) tumor suppressor. miR-494 inhibition in human HCC cell lines decreases cellular transformation and anti-miR-494 treatment of primary MYC-driven liver tumor formation significantly diminishes tumor size. Our findings identify a new therapeutic target, miR-494, for the treatment of HCC.

Keywords

HCC; cancer; cell cycle; Dlk1-Dio3; miRNA therapy

INTRODUCTION

Hepatocellular carcinoma (HCC) is the third most common cause of cancer related death worldwide [1]. Genomic alterations and subsequent aberrant activation of multiple signaling cascades make HCC a complex and heterogeneous disease [2]. MYC and RAS are canonical oncogenes whose increased expression or pathway activation has been identified in many human cancers including HCC. MYC is amplified or overexpressed in up to 70% of viral and alcohol-related HCC, while RAS pathway activation is seen in up to 89% of human HCC [3,4]. Together, their co-activation has been associated with a more proliferative phenotype and worse survival in human HCC [5].

Although extensive effort has been devoted to understanding the molecular pathogenesis of HCC, few effective treatments currently exist. Systemic chemotherapy and radiotherapy, two conventional cancer therapies, have low response rates and no demonstrated survival benefits in HCC [6]. Treatment with sorafenib, a recently approved multi-kinase inhibitor, resulted in only modestly prolonged survival [7]. Development of novel therapeutics for the prevention and treatment of HCC is therefore urgently needed.

Despite the general lack of activity of conventional therapeutics in HCC, hepatocytes have been shown to readily take up antisense oligonucleotides [8], raising the hope that small nucleic acid based molecules may have utility against HCC. miRNAs are small, endogenous RNAs that regulate gene expression through mRNA degradation or inhibition of translation [9]. Aberrant miRNA expression plays an essential role in HCC pathogenesis, and miRNA replacement or inhibition therapies have been suggested as potential therapeutics for HCC [10]. As proof of principle, recombinant AAV mediated overexpression of miR-26a was recently shown to attenuate primary MYC-driven tumor formation in a transgenic mouse model [11]. However, safety considerations exist over the clinical application of AAV-vector based gene therapy [12]. The use of drug-like antimiR oligonucleotides to inhibit miRNAs overexpressed in liver cancer may provide a robust and safer approach for the treatment of HCC. miRNA antagonists have demonstrated efficacy in tumor xenograft studies, metabolic disease and antiviral therapy [13–15]. However, whether miRNA antagonists will have therapeutic utility against primary liver tumor formation and which miRNAs should be targeted to block tumor growth remains largely unexplored.

We sought to model human HCC *in vivo* by liver-specific activation of oncogenic pathways driven by MYC and/or RAS in mice. We postulated that miRNAs upregulated in these models could be potential therapeutic targets in HCC. We find miR-494 is upregulated in multiple HCC tumor models and human HCC samples. Increased miR-494 expression promotes proliferation in tumor cells and its inhibition reduces transformation of human HCC cells and tumor growth *in vivo*, raising its potential as a therapeutic target in HCC.

EXPERIMENTAL PROCEDURES

Mouse Strains

TRE-RASV12 mice [16] were crossed with Liver Enriched Activator Protein promoter controlled tetracycline transactivator (LAP-tTA) mice [17], to generate LAP-tTA/TRE-RAS (LT2/RAS) transgenic mice. LAP-tTA/TRE-MYC (LT2/MYC) transgenic mice have been described previously [18]. LT2/MYC males were crossed with LT2/RAS females to generate LAP-tTA/TRE-MYC/TRE-RAS (LT2/MYC/RAS) mice. Doxycycline was supplied in feed (200 mg/kg) to suppress oncogene expression and removed after 8 weeks of age to induce transgene expression. The Committee for Animal Research at the University of California, San Francisco, approved all animal experiments.

Microarray Analysis

RNA from normal liver (LT2) and tumor tissue (LT2/MYC, LT2/RAS, LT2/MYC/RAS) was extracted, enriched for miRNAs and biotin-labeled using Ambion's miRVana, flashPAGE and miRVana miRNA labeling kits, respectively. Samples (n=4) from each genotype were hybridized to a custom Affymetrix Genechip designed to miRNA probes derived from Sanger miRBase v9.2. This array contained a total of 14216 probes. Mouse probes and human probes whose sequence is complementary to mouse homologs were used for the analysis. For each probe, an estimated background value was subtracted that was derived from the median signal of a set of GC-matched anti-genomic controls. Detection calls were based on a Wilcoxon rank-sum test of the miRNA probe signal compared to the distribution of signals from GC-content matched anti-genomic probes and normalized according to the variance stabilization method described [19]. Post-normalized data scale is reported as generalized $\log_2$ data. For statistical hypothesis testing, one-way ANOVA was applied and probes are considered significantly differentially expressed based on a default p-value of 0.05 and $\log_2$ difference >1 or <−1. The microarray data has been deposited at the NCBI GEO repository under accession number GSSE44570.

Human Datasets

Human HCC expression datasets were retrieved from the Gene Expression Omnibus (http://www.ncbi.nlm.nih.gov/geo/) for the Burchard set (GSE22058) and The Cancer Genome Atlas (http://cancergenome.nih.gov/). The Burchard set was based on microarray based data across 192 samples containing paired tumor and non-tumor adjacent control tissues [20]. The TCGA LIHC set was based on next-gen sequencing of 103 samples containing 67 tumors and 36 unpaired non-tumor liver tissues.

Bioinformatic Analysis

The Burchard HCC array data was quality-controlled for outliers and possible batch-effects using principal component analysis (PCA). Outliers were removed and the remaining samples were then log-transformed. The samples were then compared between tumors and non-tumor controls using one-way ANOVA. Fold changes and raw p-values were used to filter the differentially expressed miRNAs. Statistical analysis, Venn comparisons, and visualization of expression heatmaps were performed using ArrayStudio (Omicsoft) and R. The TCGA LIHC dataset was first normalized within each sample by dividing raw count values by total counts [21]. The samples were then quality controlled by PCA and subsequently log-transformed. Comparisons and visualization were also made by one-way ANOVA using similar fold change and p-value filters as with the Burchard set [20].

Please see Supplementary Experimental Procedures for additional methods.

RESULTS

MYC and/or RAS Driven Liver Tumors Have Distinct Characteristics

To model HCC in the mouse, we utilized a liver-specific doxycycline regulated oncogene expression approach[18,24]. This system allows temporal control over the expression of MYC specifically in the liver, resulting in murine liver tumor formation (LT2/MYC) [18,24]. In the present study we developed a new HRASV12-driven model of liver cancer (LT2/RAS) and also co-expressed MYC and HRASV12 together to drive liver tumor formation by both oncogenes (LT2/MYC/RAS). Adult mice of each genotype were taken off doxycycline at 8 weeks to induce oncogene expression. Transgenic mouse models gave rise to liver tumors with near 100% penetrance within a range of 5–12 weeks. To determine if specific oncogene expression resulted in distinct tumor types, we characterized livers from the four genotypes. Oncogene expression was confirmed by western blot analysis of tumor tissue (Supplementary Figure 1A). LT2 controls had normal appearing livers while MYC and RAS oncogenes induced morphologically distinct liver tumors (Figure 1A). Likewise, combined expression of MYC and RAS gave rise to heterogeneous tumors morphologically distinct from either oncogene alone (Figure 1A). Histological analysis revealed that MYC-driven tumors resemble poorly differentiated HCCs or human hepatoblastomas[25], while RAS-driven tumors resemble human HCC. MYC+RAS driven tumors are reminiscent of an aggressive variant of HCC or fetal variants of human hepatoblastoma (Figure 1B and Supplementary Figure 1B).

Alfa-fetoprotein (AFP) is expressed in fetal liver progenitors but not in normal adult liver and is used as a clinical biomarker to confirm the diagnosis of HCC[26]. We examined expression of AFP in the transgenic tumor models, and found high expression of AFP in all samples for each genotype but undetectable levels in non-tumor control mice (Figure 1C). These results confirm that while distinct, each of the transgenic models represents *bona-fide* liver tumors.

A miRNA megacluster on mouse chromosome 12qF1 is upregulated in multiple HCC models

While MYC and RAS play important roles in HCC, little is known about the effect these canonical oncogenes exert individually and together on miRNA expression. To identify aberrantly expressed miRNAs, we performed a miRNA microarray on samples collected from MYC, RAS and MYC+RAS liver tumors and compared to control (LT2) livers. We observed at least 2 fold up or down-regulation ($-1 > \log_2 > 1$ and $p < 0.05$) for 103 miRNAs in the LT2/RAS, 129 in the LT2/MYC and 118 in the LT2/MYC/RAS models compared to normal LT2 mice (Figure 2A, Supplementary Table 1). We hypothesized that the subset of miRNAs commonly deregulated in all three tumor genotypes might be especially important for HCC development. We found 60 miRNAs up (n=58) or downregulated (n=2) amongst all three genotypes compared to normal liver (intersection of the three genotypes in the venn-diagram, Figure 2A and Supplementary Table 1). To determine if the miRNA expression changes observed in these transgenic liver cancer models are relevant to human HCC, we used the shared 60-miRNA signature found in our models to cluster human HCC patient samples (Figure 2B–C). We applied the 60-miRNA liver cancer signature to two human HCC miRNA data sets and found that the signature clustered 21% (Dataset #1) and 25% (Dataset #2) of tumor samples (Figure 2B–C). Elevated tumor AFP expression has been associated with poorly differentiated and aggressive HCCs[27]. Since clinical or pathologic characteristics for these human datasets were not available, we instead examined tumor AFP mRNA expression to determine if it differed between tumor samples clustered by the 60-miRNA signature. In both datasets, we found significantly increased tumor AFP expression in the tumor samples clustered by the 60-miRNA signature (Figure 2D–E). Thus

the 60-miRNA signature shared amongst all mouse liver tumor models, can distinguish human tumors associated with elevated AFP expression, a marker of poorly differentiated state.

Since previous studies have demonstrated that clusters of miRNAs can play important roles in development, disease and cancer [28–30], we sought to determine if the 58 upregulated miRNAs were clustered within the genome. Surprisingly, 29 of the 58 (50%) commonly upregulated miRNAs are located in the same genomic locus on mouse chromosome 12qF1 (Figure 2F). This region, known as the Dlk1-Dio3 domain, is conserved among placental mammals and comprises approximately 5% of all known miRNA genes[31]. miRNAs from the Dlk1-Dio3 region are split into two separate clusters, which we termed the Anti-Rtl1 and Mirg clusters, respectively (Supplementary Figure 2).

We next asked if this miRNA megacluster is also upregulated in other models of liver cancer. An unbiased *Sleeping Beauty* transposon system generates liver cancer in mice at ~35% frequency[22]. Pyrosequencing of liver tumors from these mice revealed a preferential transposon integration site within the Anti-Rtl1 cluster in 73% (8/11) of samples. Five of these eight tumors had transposon integrations in the same transcriptional orientation resulting in significant upregulation of Dlk1-Dio3 miRNAs (Figure 2G). Together, these results suggest that upregulation of miRNAs within the Dlk1-Dio3 megacluster may promote HCC development in mice.

miR-494 enhances transformation of liver tumor cells and is upregulated in human HCC

Studies of oncogenic miRNA clusters suggest that only one or a few miRNAs may account for the tumor-promoting properties of these clusters[32]. To identify such miRNAs within the Dlk1-Dio3 megacluster, we tested their ability to accelerate cell growth in soft agar. We split the Dlk1-Dio3 megacluster into 13 subclusters and stably expressed each in a mouse liver tumor cell line (Supplementary Figure 3A and Supplementary Table 3). LT2MR cells, derived from LT2/MYC tumors and engineered to stably express RAS (Supplementary Figure 3B), showed reduced or absent expression of many Dlk1-Dio3 miRNAs (data not shown), making it a suitable system to assess the effects of overexpression of miRNAs within the megacluster. Stable expression was verified by quantitative real-time PCR (qRT-PCR) of a representative miRNA within each subcluster (Supplementary Figure 3C). We found four subclusters of miRNAs that significantly increased LT2MR colony growth in soft agar. However, we were most intrigued by the observation that subclusters SM-4 and SM-5, each containing a single miRNA (miR-494 and -495, respectively), were the most potent at increasing soft agar growth (Figure 2H).

miR-494 and miR-495 were highly upregulated in all three tumor genotypes as verified by qRT-PCR (Supplementary Table 2, Supplementary Figure 4). To investigate if these miRNAs might also be upregulated in human HCC, we performed qRT-PCR on 47 human HCC samples and their matched normal tissues. 34% (n=16) and 27% (n=13) of samples had >1.5 fold miR-494 and miR-495 overexpression compared to normal liver tissue, respectively (Figure 2I). miR-494 and miR-495 were also part of the 60-miRNA signature found to be up-regulated in dataset #2 (Figure 2C). Because miR-494 was more frequently upregulated in primary human HCC samples, we selected it for further study.

miR-494 Overexpression Increases Cellular Proliferation and S-Phase Entry

Since miR-494 was amongst the most potent at increasing soft agar growth, we determined if it could directly effect tumor cell proliferation. To address this, we performed proliferation assays on LT2MR cells stably overexpressing miR-494 (Supplementary Figure 5). We observed that miR-494 overexpression increased LT2MR proliferation compared to control

cells. Conversely, stable expression of a miR-494 antagonist resulted in diminished miR-494 expression (Supplementary Figure 5) and attenuated proliferation of LT2MR cells compared to controls (Figure 3A).

We asked if the observed increase in proliferation was mediated through alterations in cell cycle control and performed DNA content analysis of LT2MR cells. miR-494 mimic transfection resulted in decreased G1-phase and increased S-phase cells (Figure 3B) while miR-494 inhibitor transfection resulted in increased G1-phase and decreased S-phase cells (Figure 3B). These results suggest that miR-494 could play a role in G1/S transition in LT2MR cells. We next treated cells with bromodeoxyuridine (BrdU) and measured its incorporation. We observed that miR-494 mimic transfection caused an increase in S-phase BrdU labeled cells, while miR-494 inhibitor transfection resulted in decreased S-phase BrdU labeled cells (Figure 3C).

We next examined if increased S-phase entry caused by miR-494 was associated with changes in the expression of cell cycle inhibitor proteins. Thus, we tested for expression of two key regulators of the G1/S transition, p21 and p27, and observed decreased expression of both in miR-494 overexpressing cells (Figure 3D). In contrast, miR-494 knockdown increased the expression of these cell cycle inhibitors (Figure 3D). We confirmed these findings in a separate cell line, Hepa1-6 mouse hepatoma cells, which have high miR-494 expression. miR-494 inhibition decreased proliferation in Hepa1-6 cells, associated with a delay in G1/S transition and an increase in p21 and p27 (Supplementary Figure 6A–E). Together, these results demonstrate that miR-494 overexpression increases G1/S transition in LT2MR and Hepa1-6 cells, and is associated with decreased p21 and p27 abundance, known inhibitors of cell proliferation.

The Tumor Suppressor MCC is a Direct Target of miR-494

We hypothesized miR-494 may regulate one or more growth inhibitory genes to alter cell proliferation. We identified seven candidate miR-494 targets using Targetscan, previously established to block cell cycle progression, and also containing conserved miR-494 binding sites: TACC2, TGFB2, RB1, RB1CC1, CDC73, WEE1 and MCC. To evaluate if these genes were direct miR-494 targets, we cloned a fragment of their 3′ UTRs containing the putative miR-494 binding sites into luciferase reporter constructs. MiR-494 had negligible effect on the RB1, RB1CC1, CDC73 and WEE1 UTRs, and increased TACC2 and TGFB2 UTR reporter expression (Supplementary Figure 7). However, we observed a 70% decrease in reporter expression when the MCC (Mutated in Colorectal Cancer) 3′ UTR reporter was co-transfected with miR-494 mimic, and a 40% increase in reporter expression when transfected with miR-494 inhibitor (Figure 4B). The 5203bp MCC 3′ UTR contains one 7-mer binding site for miR-494 (seed region 5049–5055nt) conserved among human, mouse and chimpanzee transcripts (Figure 4A). To determine if MCC was indeed a miR-494 target, we mutated four nucleotides within the putative seed-binding site. Reporter responsiveness was abrogated when this mutant reporter was co-transfected with either a miR-494 mimic or miR-494 inhibitor (Figure 4B).

We next examined if miR-494 altered endogenous MCC expression. To test this, we first compared the expression of MCC mRNA in LT2MR cells transfected with either miR-494 mimic or inhibitor. In mimic transfected cells, we detected a 60% decrease in MCC mRNA abundance. Conversely, MCC mRNA was significantly increased in inhibitor-transfected cells (Figure 4C). We further analyzed protein expression of MCC in mimic and inhibitor transfected cells by western blot. Consistent with MCC mRNA expression changes, we observed an 80% decrease in MCC protein expression with mimic transfected cells and a 60% increase in expression with antimiR transfected cells (Figure 4D). Transfection of

miR-494 antimiR also increased MCC protein expression in Hepa1-6 cells (Supplementary Figure 6D). Collectively, these results indicate that MCC is a direct target of miR-494.

MCC modulates G1/S transition in liver tumor cells

To assess if MCC knockdown could mimic the proliferative effect of miR-494, we silenced its expression in LT2MR cells by RNA interference. Similar to miR-494 overexpression, MCC knockdown caused increased proliferation over four days (Figure 5A), accompanied by increased G1/S transition (Figure 5B, C). Conversely, MCC overexpression caused decreased cell proliferation (Figure 5A), and was associated with delayed G1/S transition. This was consistent with observations made in cells with reduced miR-494 levels (Figure 3B, C). We next asked if MCC was altering p21 and p27 levels, similar to miR-494. From western blot analysis, we observed an alteration in p27 but not p21 protein expression when cells were transfected with either MCC siRNA or MCC cDNA (Figure 5D). This suggests that the G1/S delay caused by MCC increases p27 expression. However, other targets of miR-494 might be involved in suppressing p21 expression independently of MCC. We next asked if G1/S transition delay caused by miR-494 knockdown could be rescued by reducing MCC levels. To address this, we assessed BrdU incorporation in cells co-transfected with miR-494 antagonist and MCC siRNA. Accordingly, G1/S transition delay caused by miR-494 knockdown was reversed by co-transfection of MCC siRNA (Figure 5E). Together, these results indicate that miR-494 causes increased proliferation in LT2MR cells through suppression of MCC expression.

The role of MCC in human HCC is poorly understood, although a recent study indicated that it can be silenced by retrotransposon insertions in a subset of patients, suggesting a role as a tumor suppressor in liver cancer[33]. We examined the mRNA expression of MCC from two human datasets in which the expression of non-tumor liver tissue was also available and found that MCC was dramatically down-regulated in tumors, consistent with its role as a tumor suppressor in HCC (Figure 6A). While there may be multiple mechanisms to attenuate MCC expression in HCC, the present study demonstrates that miR-494 is one such way to directly target MCC.

miR-494 Knockdown Decreases Transformation of Human HCC Cells

Since our prior observations were made in mouse cells, we wondered if miR-494 had similar effects in a human context. To test this, we knocked-down miR-494 expression in two human HCC cell lines (Huh7 and Hep3B, with elevated miR-494 expression (Supplementary Figure 8A). Stable miR-494 inhibition was accompanied by increased MCC and p27 expression (Figure 6B). To assess the effects of miR-494 inhibition on transformation, we performed soft agar colony formation assays and scored the number of colonies formed after two weeks. We observed a significant decrease in colony formation in cells with miR-494 inhibition (Figure 6C). These results indicate that reduction of miR-494 expression increases MCC expression and impairs transformation in human HCC cells.

In Vivo Delivery of a miR-494 Antagonist Attenuates Liver Tumor Formation

Since miR-494 inhibition resulted in diminished proliferation, we reasoned that this might decrease primary tumor formation *in vivo*. To test this, we initiated *de novo* liver tumor formation in LT2/MYC mice and treated them with either antimiRs against miR-494 or a scrambled sequence. Reduction in miR-494 expression was confirmed by qRT-PCR performed on tumor tissue (Supplementary Figure 8B). After three weeks, we observed a significantly decreased tumor burden in mice treated with miR-494 antimiR (Figure 6D, E). We next asked if miR-494 inhibition affected MCC expression *in vivo*. We observed an increase in both MCC and p27 protein expression in tumors of antimiR-494 treated mice (Figure 6F, G). TUNEL staining revealed that there was no significant difference in

apoptosis following either treatment, suggesting that miR-494 acts through attenuated cell proliferation rather than increased apoptosis (Supplementary Figure 8C). Our results indicate that knockdown of miR-494 with a drug-like antagonist can significantly diminish primary HCC tumor formation.

DISCUSSION

The affinity of hepatocytes for small nucleic acids suggests miRNA antagonist-based therapy might be a promising approach. In this study, we characterized oncogene-specific miRNA expression changes in *de novo* tumor formation. We report, for the first time, miRNA expression changes associated with liver tumor formation driven by MYC, RAS and MYC+RAS oncogenes. We find that miR-494 is upregulated, as part of a miRNA megacluster, in multiple mouse tumor models and clinical human HCC samples. We show that it plays a role in regulating the cell cycle through MCC, and demonstrate the therapeutic potential of targeting miR-494 in both human HCC cell lines and *de novo* tumors.

The common upregulation of a large megacluster of miRNAs from the Dlk1-Dio3 locus in all three of our liver tumor models was initially surprising to us. However, recent studies have highlighted the increasing importance of this locus in HCC[12,22,34–36]. The convergence of these data suggests that Dlk1-Dio3 miRNAs could play an important role in HCC development. In our study, we dissected this cluster in a systematic manner, and identified miR-494 as a therapeutic target in HCC. However, our results indicate that other oncogenic miRNAs within this megacluster also play a role in cellular transformation (Figure 2H). For example, another miRNA from this locus has been shown to be oncogenic in neurobalstoma[37]. Whether other Dlk1-Dio3 miRNAs are also crucial to liver tumor formation and could be useful targets for therapy remains to be determined. Interestingly, we find that inhibition of miR-494 can substantially inhibit primary tumor growth, demonstrating its importance as a therapeutic target for HCC.

The role of miR-494 in tumor development appears to be tissue dependent, causing increased proliferation in H460 lung cancer cells and breast and transformed bronchial epithelial cells[38–40]. However, it induces cell cycle arrest in lung cancer and cholangiocarcinoma[41,42]. Our results demonstrate that miR-494 increases proliferation in HCC through an acceleration of G1/S transition, but the pleiotropic nature of miRNAs suggests that it could have additional gene targets, which may play other roles in tumorigenesis. miR-494 has been found to target PTEN[38], and we investigated this in the context of our tumor models. While we were unable to detect PTEN downregulation when miR-494 was overexpressed in LT2MR cells (data not shown), we found that miR-494, targets the tumor suppressor MCC. Importantly, loss of MCC in HCC was also recently found to occur in a subset of human tumors through inactivating insertion of LINE-1 retrotransposon elements [33]. Our study supports the role of MCC as a *bona fide* tumor suppressor in HCC that can be a direct target of an oncogenic miRNA. As with other tumor suppressors, it is likely that miR-494 over-expression and LINE-1 insertions may represent just two possible mechanisms to inactivate MCC in liver cancer. Furthermore, although we did not find other candidate tumor suppressor genes as miR-494 targets (Supplementary Figure 7), we do not rule out the possibility of them being targets in other cell types, or that miR-494 could have other tumor suppressor targets in HCC.

Most prior *in vivo* studies aimed at modulating miRNA expression have been performed using orthotopic transplant models[10,15]. The data generated from these models is promising and will no doubt remain a fruitful area of research. However, we felt that treatment of liver tumors, as they form, with a miRNA antagonist would more closely replicate the clinical paradigms in which such therapies could eventually be employed. To this end, we took

advantage of LT2/MYC mice, with the ability to form *de novo* liver tumors driven by MYC. In this same model, AAV based overexpression of miR-26a, a tumor suppressive miRNA in HCC, was previously shown to diminish tumor growth[11]. To our knowledge, we are the first to demonstrate that therapeutic delivery of a miRNA antagonist is successful at limiting the growth of *de novo* liver tumors. These findings represent a significant step toward the use of antimiR based therapy *in vivo*, and indicate that the delivery of antagonists against other highly upregulated miRNAs, such as miR-21 and 221, could be a promising therapeutic approach in HCC[43,44]. The present study highlights the therapeutic potential of targeting miRNAs such as miR-494 in HCC.

Supplementary Material

Refer to Web version on PubMed Central for supplementary material.

Acknowledgments

Financial Support:

The work was supported by fellowship supported by A*STAR (L.L.) and by the Susan G. Komen Foundation (A.G.), N.I.H. CA136717 and CA170447 (A.G.), UCSF Program for Breakthrough Biological Research and a V-Foundation award (A.G.) and UCSF Liver Center (P30 DK026743).

We thank Mercedes Joaquin for technical assistance, Eric Marcusson (Regulus Therapeutics) for kindly providing miR-494 antagonists and controls, and the TCGA Research Network for generating the TCGA LIHC datasets.

List of abbreviations

HCC	Hepatocellular carcinoma
miRNA	MicroRNAs
MCC	Mutated in Colorectal Cancer
UTR	Untranslated region
mRNA	Messenger RNA
AAV	Adeno-Associated Virus
LAP	Liver enriched activator protein
SB	Sleeping Beauty
LM-PCR	Ligation-mediated PCR
AFP	Alpha-fetoprotein
DAVID	Database for Annotation, Visualization and Integrated Discovery
TACC2	Transforming, acidic coiled-coil containing protein 2
TGFB2	Transforming growth factor, beta 2
RB1	Retinoblastoma 1
RB1CC1	Retinoblastoma 1 inducible coiled-coil 1
CDC73	Cell division cycle 73
Id3	Inhibitor of DNA binding 3
APC	Adenomatous polyposis coli

References

1. Bosch FX, Ribes J, Diaz M, et al. Primary liver cancer: worldwide incidence and trends. Gastroenterology. 2004; 127:S5–S16. [PubMed: 15508102]
2. Schlaeger C, Longerich T, Schiller C, et al. Etiology-dependent molecular mechanisms in human hepatocarcinogenesis. Hepatology. 2008; 47:511–520. [PubMed: 18161050]
3. Gan FY, Gesell MS, Alousi M, et al. Analysis of ODC and c-myc gene expression in hepatocellular carcinoma by in situ hybridization and immunohistochemistry. J Histochem Cytochem. 1993; 41:1185–1196. [PubMed: 7687263]
4. Newell P, Toffanin S, Villanueva A, et al. Ras pathway activation in hepatocellular carcinoma and anti-tumoral effect of combined sorafenib and rapamycin in vivo. J Hepatol. 2009; 51:725–733. [PubMed: 19665249]
5. Calvisi DF, Ladu S, Gorden A, et al. Ubiquitous activation of Ras and Jak/Stat pathways in human HCC. Gastroenterology. 2006; 130:1117–1128. [PubMed: 16618406]
6. Llovet JM, Bruix J. Molecular targeted therapies in hepatocellular carcinoma. Hepatology. 2008; 48:1312–1327. [PubMed: 18821591]
7. Llovet JM, Ricci S, Mazzaferro V, et al. Sorafenib in advanced hepatocellular carcinoma. N Engl J Med. 2008; 359:378–390. [PubMed: 18650514]
8. Zimmermann TS, Lee AC, Akinc A, et al. RNAi-mediated gene silencing in non-human primates. Nature. 2006; 441:111–114. [PubMed: 16565705]
9. He L, Hannon GJ. MicroRNAs: small RNAs with a big role in gene regulation. Nat Rev Genet. 2004; 5:522–531. [PubMed: 15211354]
10. Braconi C, Patel T. Non-coding RNAs as therapeutic targets in hepatocellular cancer. Curr Cancer Drug Targets. 2012; 12:1073–1080. [PubMed: 22873215]
11. Kota J, Chivukula RR, O'Donnell KA, et al. Therapeutic microRNA delivery suppresses tumorigenesis in a murine liver cancer model. Cell. 2009; 137:1005–1017. [PubMed: 19524505]
12. Donsante A, Miller DG, Li Y, et al. AAV vector integration sites in mouse hepatocellular carcinoma. Science. 2007; 317:477. [PubMed: 17656716]
13. Elmen J, Lindow M, Silahtaroglu A, et al. Antagonism of microRNA-122 in mice by systemically administered LNA-antimiR leads to up-regulation of a large set of predicted target mRNAs in the liver. Nucleic Acids Res. 2008; 36:1153–1162. [PubMed: 18158304]
14. Lanford RE, Hildebrandt-Eriksen ES, Petri A, et al. Therapeutic silencing of microRNA-122 in primates with chronic hepatitis C virus infection. Science. 2010; 327:198–201. [PubMed: 19965718]
15. Park JK, Kogure T, Nuovo GJ, et al. miR-221 silencing blocks hepatocellular carcinoma and promotes survival. Cancer Res. 2011; 71:7608–7616. [PubMed: 22009537]
16. Chin L, Tam A, Pomerantz J, et al. Essential role for oncogenic Ras in tumour maintenance. Nature. 1999; 400:468–472. [PubMed: 10440378]
17. Kistner A, Gossen M, Zimmermann F, et al. Doxycycline-mediated quantitative and tissue-specific control of gene expression in transgenic mice. Proc Natl Acad Sci U S A. 1996; 93:10933–10938. [PubMed: 8855286]
18. Shachaf CM, Kopelman AM, Arvanitis C, et al. MYC inactivation uncovers pluripotent differentiation and tumour dormancy in hepatocellular cancer. Nature. 2004; 431:1112–1117. [PubMed: 15475948]
19. Huber W, von Heydebreck A, Sultmann H, et al. Variance stabilization applied to microarray data calibration and to the quantification of differential expression. Bioinformatics. 2002; 18 (Suppl 1):S96–104. [PubMed: 12169536]
20. Burchard J, Zhang C, Liu AM, et al. microRNA-122 as a regulator of mitochondrial metabolic gene network in hepatocellular carcinoma. Mol Syst Biol. 2010; 6:402. [PubMed: 20739924]
21. Fehniger TA, Wylie T, Germino E, et al. Next-generation sequencing identifies the natural killer cell microRNA transcriptome. Genome Res. 2010; 20:1590–1604. [PubMed: 20935160]
22. Dupuy AJ, Rogers LM, Kim J, et al. A modified sleeping beauty transposon system that can be used to model a wide variety of human cancers in mice. Cancer Res. 2009; 69:8150–8156. [PubMed: 19808965]

23. Horiuchi D, Kusdra L, Huskey NE, et al. MYC pathway activation in triple-negative breast cancer is synthetic lethal with CDK inhibition. J Exp Med. 2012; 209:679–696. [PubMed: 22430491]
24. Goga A, Yang D, Tward AD, et al. Inhibition of CDK1 as a potential therapy for tumors over-expressing MYC. Nat Med. 2007; 13:820–827. [PubMed: 17589519]
25. Cairo S, Armengol C, De Reynies A, et al. Hepatic stem-like phenotype and interplay of Wnt/beta-catenin and Myc signaling in aggressive childhood liver cancer. Cancer Cell. 2008; 14:471–484. [PubMed: 19061838]
26. Abou-Alfa GK, Venook AP. The impact of new data in the treatment of advanced hepatocellular carcinoma. Curr Oncol Rep. 2008; 10:199–205. [PubMed: 18765149]
27. Yamashita T, Forgues M, Wang W, et al. EpCAM and alpha-fetoprotein expression defines novel prognostic subtypes of hepatocellular carcinoma. Cancer Res. 2008; 68:1451–1461. [PubMed: 18316609]
28. He L, Thomson JM, Hemann MT, et al. A microRNA polycistron as a potential human oncogene. Nature. 2005; 435:828–833. [PubMed: 15944707]
29. O'Donnell KA, Wentzel EA, Zeller KI, et al. c-Myc-regulated microRNAs modulate E2F1 expression. Nature. 2005; 435:839–843. [PubMed: 15944709]
30. Stadtfeld M, Apostolou E, Akutsu H, et al. Aberrant silencing of imprinted genes on chromosome 12qF1 in mouse induced pluripotent stem cells. Nature. 2010; 465:175–181. [PubMed: 20418860]
31. Cavaille J, Seitz H, Paulsen M, et al. Identification of tandemly-repeated C/D snoRNA genes at the imprinted human 14q32 domain reminiscent of those at the Prader-Willi/Angelman syndrome region. Hum Mol Genet. 2002; 11:1527–1538. [PubMed: 12045206]
32. Olive V, Bennett MJ, Walker JC, et al. miR-19 is a key oncogenic component of mir-17-92. Genes Dev. 2009; 23:2839–2849. [PubMed: 20008935]
33. Shukla R, Upton KR, Munoz-Lopez M, et al. Endogenous retrotransposition activates oncogenic pathways in hepatocellular carcinoma. Cell. 2013; 153:101–111. [PubMed: 23540693]
34. Lempiainen H, Couttet P, Bolognani F, et al. Identification of Dlk1-Dio3 imprinted gene cluster noncoding RNAs as novel candidate biomarkers for liver tumor promotion. Toxicol Sci. 2013; 131:375–386. [PubMed: 23091169]
35. Luk JM, Burchard J, Zhang C, et al. DLK1-DIO3 Genomic Imprinted MicroRNA Cluster at 14q32. 2 Defines a Stemlike Subtype of Hepatocellular Carcinoma Associated with Poor Survival. J Biol Chem. 2011; 286:30706–30713. [PubMed: 21737452]
36. Riordan JD, Keng VW, Tschida BR, et al. Identification of rtl1, a retrotransposon-derived imprinted gene, as a novel driver of hepatocarcinogenesis. PLoS Genet. 2013; 9:e1003441. [PubMed: 23593033]
37. Swarbrick A, Woods SL, Shaw A, et al. miR-380-5p represses p53 to control cellular survival and is associated with poor outcome in MYCN-amplified neuroblastoma. Nat Med. 2010; 16:1134–1140. [PubMed: 20871609]
38. Liu L, Jiang Y, Zhang H, et al. Overexpressed miR-494 down-regulates PTEN gene expression in cells transformed by anti-benzo(a)pyrene-trans-7,8-dihydrodiol-9,10-epoxide. Life Sci. 2010; 86:192–198. [PubMed: 20006626]
39. Liu Y, Lai L, Chen Q, et al. MicroRNA-494 is required for the accumulation and functions of tumor-expanded myeloid-derived suppressor cells via targeting of PTEN. J Immunol. 2012; 188:5500–5510. [PubMed: 22544933]
40. Romano G, Acunzo M, Garofalo M, et al. MiR-494 is regulated by ERK1/2 and modulates TRAIL-induced apoptosis in non-small-cell lung cancer through BIM down-regulation. Proc Natl Acad Sci U S A. 2012; 109:16570–16575. [PubMed: 23012423]
41. Ohdaira H, Sekiguchi M, Miyata K, et al. MicroRNA-494 suppresses cell proliferation and induces senescence in A549 lung cancer cells. Cell Prolif. 2012; 45:32–38. [PubMed: 22151897]
42. Olaru AV, Ghiaur G, Yamanaka S, et al. MicroRNA down-regulated in human cholangiocarcinoma control cell cycle through multiple targets involved in the G1/S checkpoint. Hepatology. 2011; 54:2089–2098. [PubMed: 21809359]
43. Connolly E, Melegari M, Landgraf P, et al. Elevated expression of the miR-17-92 polycistron and miR-21 in hepadnavirus-associated hepatocellular carcinoma contributes to the malignant phenotype. Am J Pathol. 2008; 173:856–864. [PubMed: 18688024]

44. Pineau P, Volinia S, McJunkin K, et al. miR-221 overexpression contributes to liver tumorigenesis. Proc Natl Acad Sci U S A. 2010; 107:264–269. [PubMed: 20018759]

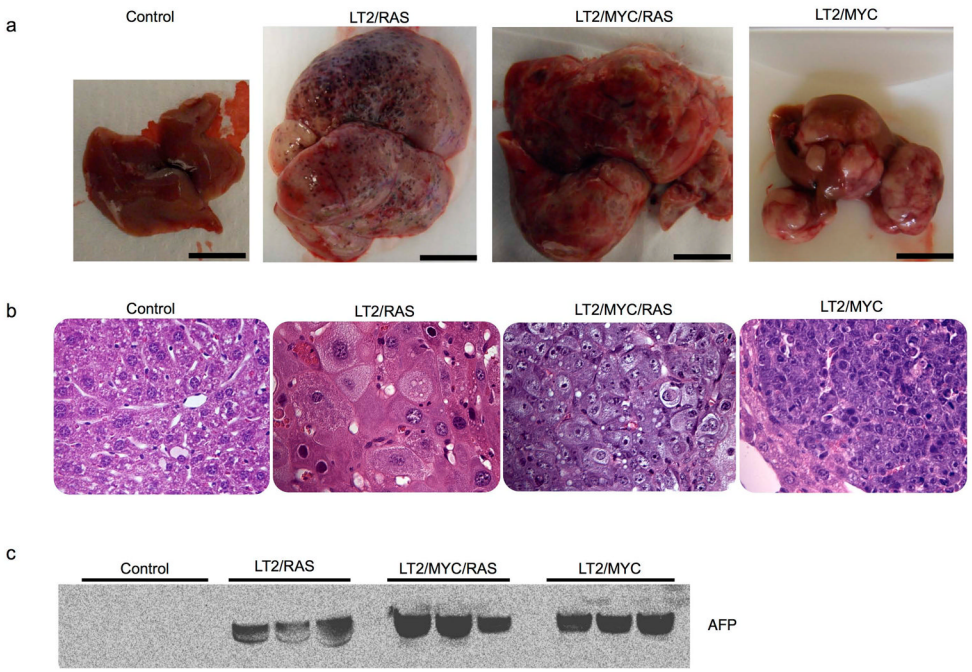

Figure 1. Doxycycline-regulated expression of MYC or/and RAS oncogenes give rise to distinct liver tumors

A. Gross morphology of representative control liver and tumors from each genotype are shown. Scale bar = 1 cm. **B.** H & E histology from representative samples for control (LT2) liver and tumors from each genotype. Original magnification = 40x. **C.** Western blot for AFP, a liver cancer marker, which is expressed at high levels in all three liver tumor models and is absent in control livers (controls). Equal amounts of total protein for each sample were loaded and verified by Ponceau-S staining.

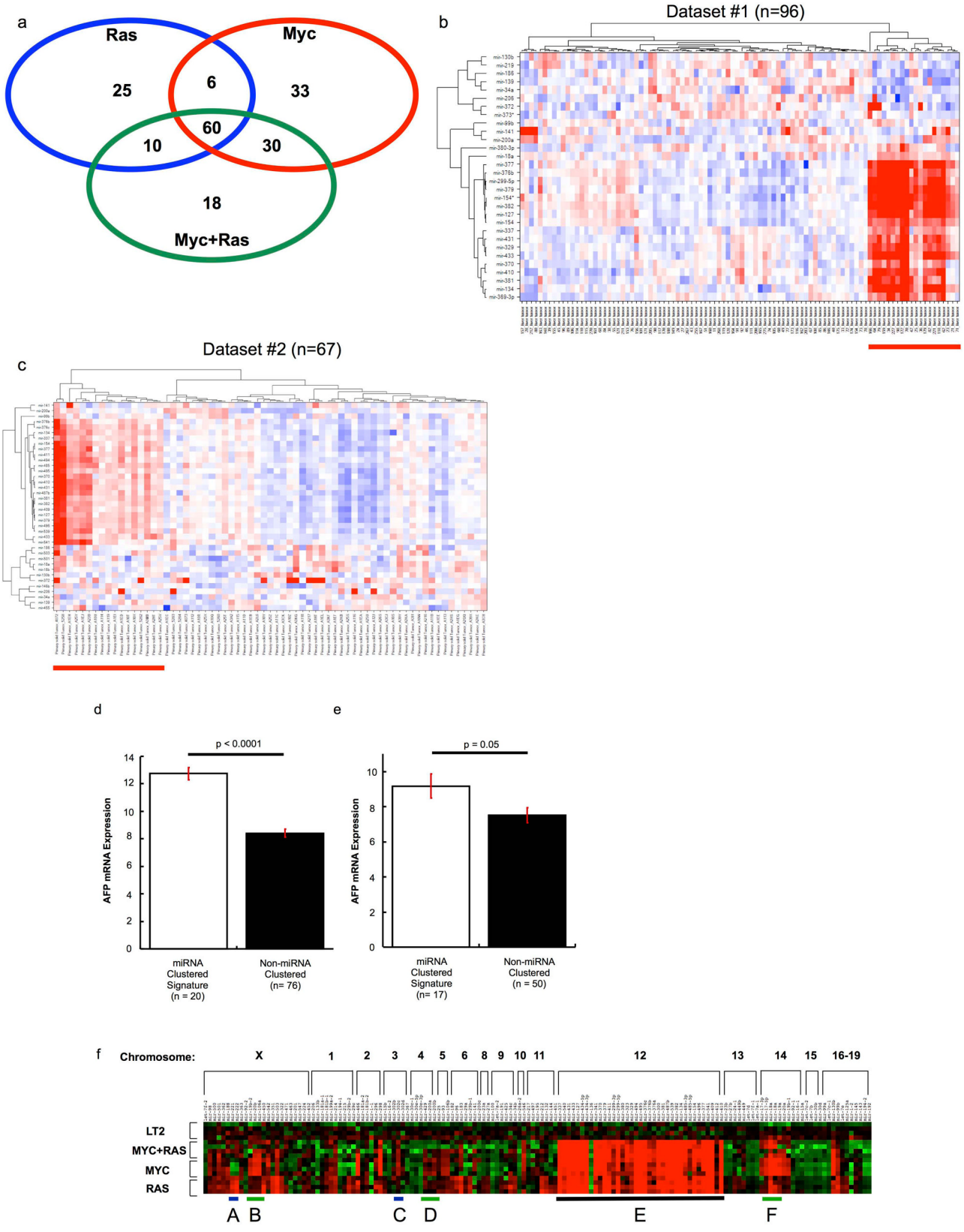

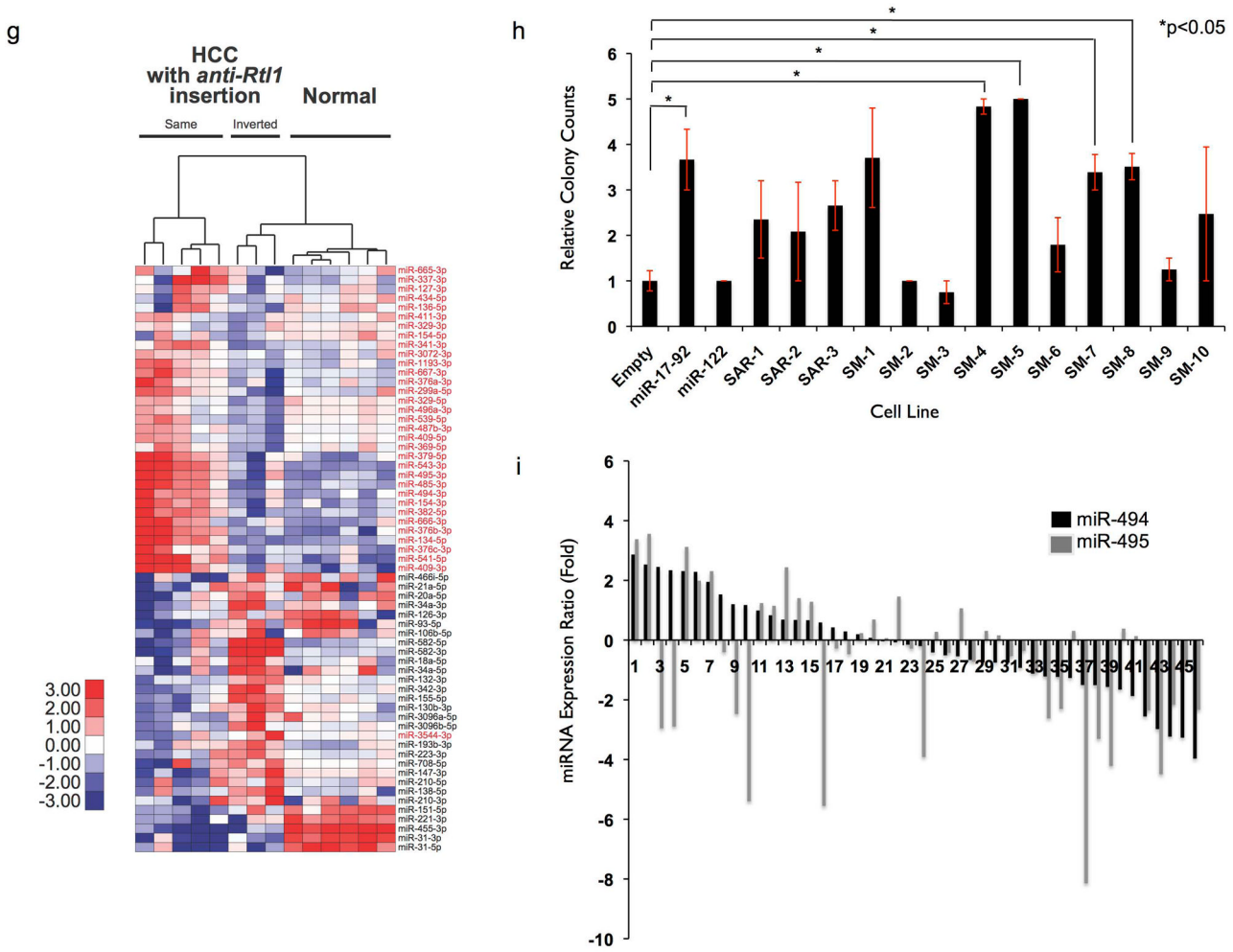

Figure 2. A miRNA megacluster containing multiple transforming miRNAs is upregulated in mouse tumor models

A. Venn analysis of differentially expressed miRNAs in MYC, RAS, and MYC+RAS transgenic mice indicate substantial overlap. MicroRNA signatures from each mouse line were performed using one-way ANOVA comparisons with a minimum fold change log 2 >1 or <−1 at a p-value <0.05. The intersection of the three signatures indicated 60 miRNAs were commonly shared among these mice. Orthologs of these miRNAs were used for subsequent analysis in human HCC cohorts. **B., C.** Distinct subsets of human HCC tumors with upregulated miRNA orthologs of the 60-miRNA murine signature. Two-dimensional unsupervised hierarchical clustering of orthologous miRNAs was performed based on miRNAs from the murine signature. **B.** 30 for Dataset#1 Ref [20] **C.** 38 for Dataset#2, TCGA LIHC. Red indicates miRNA up-regulation, blue indicates down-regulation on the heatmaps. **D., E.** AFP expression is elevated in human HCC tumors that exhibit high miRNA signature. Mean AFP mRNA expression is depicted and error bars represent S.E.M. **D.** Dataset#1, **E.** Dataset#2. **F.** Hierarchical clustering of all miRNAs located within 1kb of each other in the mouse genome reveals an upregulated megacluster on Chr12qF1 in mouse tumors (heatmap region E, underlined in black). miR-17-92 oncomiR cluster and its homologs are indicated with green lines (heatmap regions B, D and F). RAS regulated miR-221-222 cluster shows RAS specific expression (heatmap region A), while MYC regulated miR-302b-d cluster shows MYC specific expression (heatmap region C). **G.**

Sleeping beauty transposon integration in the same transcriptional orientation as the anti-Rtl1 cluster causes HCCs in mice, accompanied by an upregulation of Dlk1-Dio3 miRNAs (indicated in red). This is compared to HCCs with inverted SB insertions in the anti-Rtl1 cluster and normal livers that have no Dlk1-Dio3 miRNA upregulation. **H.** Quantification of soft agar colonies formed by each LT2MR stable cell line. miR-17-92 and miR-122 were used as positive and negative controls, respectively. Values are average of 3 independent experiments. SM-4, 5, 7 and 8 subclusters significantly increased transformation when compared to LT2MR cells stably expressing a control pMSCV vector (*$p<0.05$). **I.** Relative expression of miR-494 and miR-495 from 47 human HCC tumor and matched normal samples were analyzed by qRT-PCR. miRNA abundance was normalized to RNU48. Differences in expression are shown as fold change over matched normal tissue.

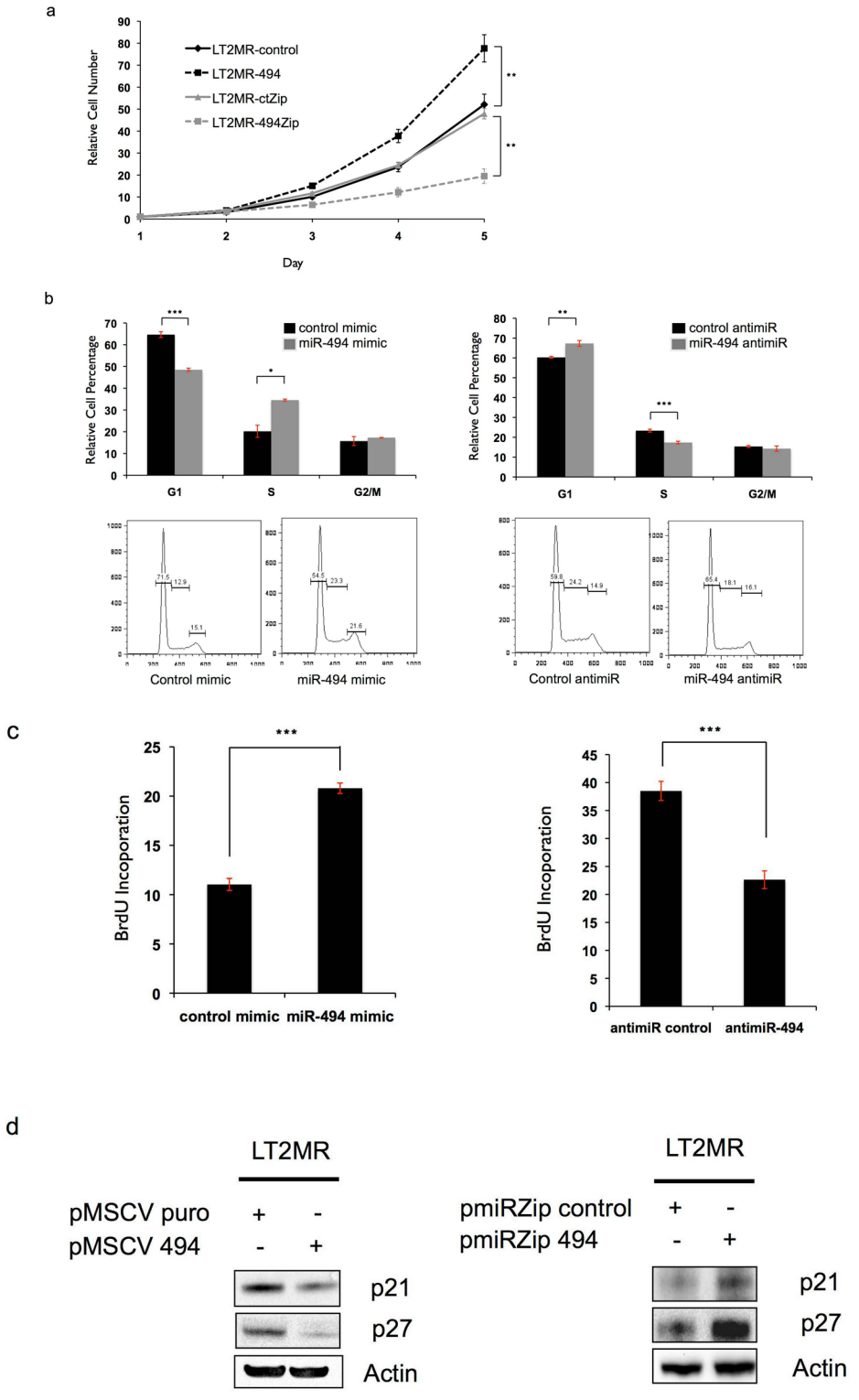

Figure 3. miR-494 increases proliferation through accelerated G1/S transition

A. LT2MR cells undergo increased proliferation with enforced miR-494 expression and decreased proliferation with miR-494 inhibition. 50,000 cells were plated in triplicate and counted at days 1, 2, 3, 4 and 5 after transfection of pMSCV puro, pMSCV 494, pmiR-ZIP-

control or pmiR-ZIP-494. Cell numbers were normalized to day 1. Experiment was repeated 3 times and values are from 1 representative experiment. **p=0.01. **B.** LT2MR cells exhibit accelerated G1/S transition with enforced miR-494 expression and G1/S delay with miR-494 inhibition. LT2MR cells transfected with miR-494 or control mimic and miR-494 or control inhibitor for 48 hours were stained with PI for FACS analysis. Cell cycle profiles were analyzed using FlowJo Analysis Software. Experiment was done with three replicates per sample and values were averaged to generate graphs (top panels). *p=0.01, **p=0.003, ***p=0.001. Figure is representative of three experiments. **C.** BrdU incorporation in miR-494 overexpressing cells. LT2MR cells were transfected with either miRNA mimics (left panel) or miRNA inhibitors (right panel) for 48h and exposed to BrdU for 40 min. Flow cytometry was used to measure BrdU incorporation. Experiment was repeated 3 times with 3 replicates per sample and values are from 1 representative experiment. ***p=0.008. **D.** Expression of cell cycle inhibitors corresponds to proliferation. Stable cell lines with either increased (left panel) or decreased miR-494 (right panel) expression were generated and tested for expression of p27 and p21 by western blot.

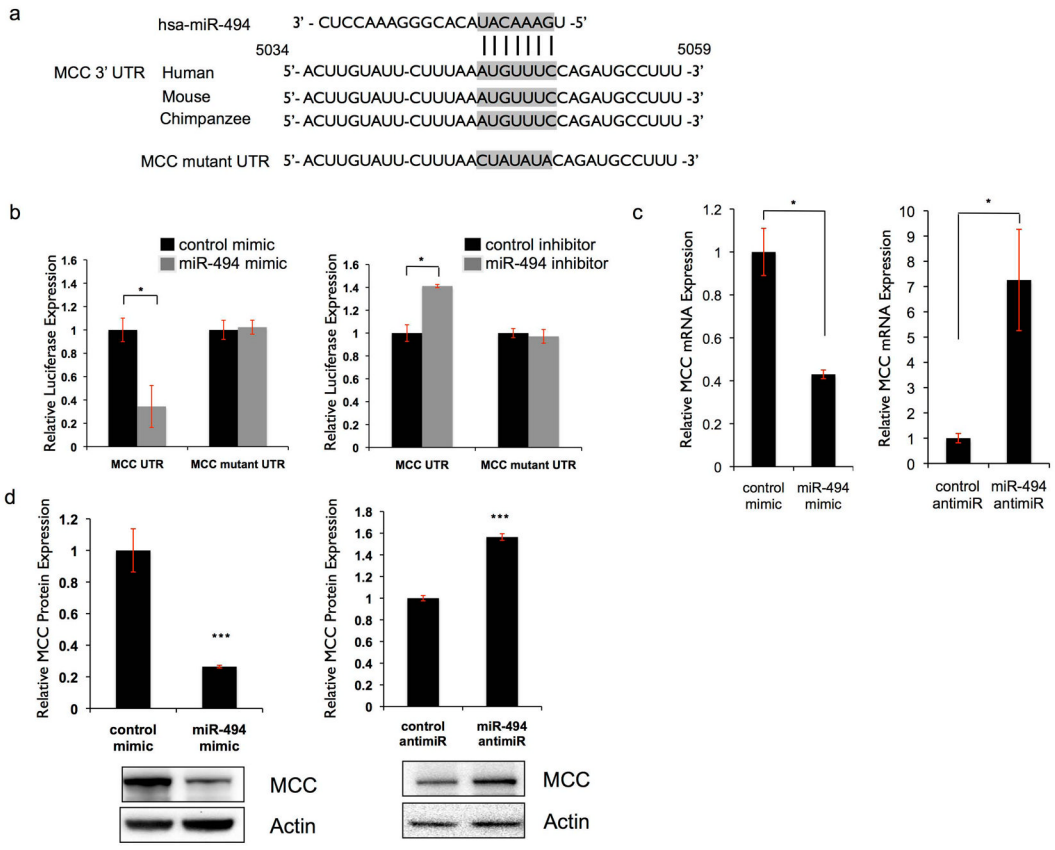

Figure 4. MCC is a direct target of miR-494

A. Putative binding site of miR-494 in MCC 3′ UTR is conserved across multiple species. Alignment of human, mouse and chimpanzee MCC 3′ UTRs shows a highly conserved region predicted to bind to miR-494. Predicted 7-mer binding seed of miR-494 to MCC 3′ UTR indicated with vertical lines. Putative binding site was mutated as indicated. **B.** MCC 3′ UTR is a direct target of miR-494. A 300bp region of the MCC 3′ UTR containing the predicted miR-494 binding site was cloned into a pMIR-REPORT luciferase vector. Activity of the reporter was decreased when co-transfected into LT2MR cells with miR-494 mimic and increased when co-transfected with miR-494 antimiR, compared to control co-transfections. *p<0.05. In both cases, site-directed mutagenesis of the predicted miR-494 binding site resulted in loss of reporter response. **C.** MCC mRNA expression is responsive to miR-494. LT2MR cells were transfected with miR-494 mimic or hairpin inhibitor and tested for MCC mRNA expression after 24h by qRT-PCR. Values normalized to sno202 and expressed relative to control transfected cells. *p<0.05. **D.** MCC protein expression is responsive to miR-494. LT2MR cells were transfected with miR-494 mimic or inhibitor and tested for MCC protein expression after 48h by western blot. Graph is an average of three independent transfections and values were quantified using a BioRad Chemidoc. ***p<0.001.

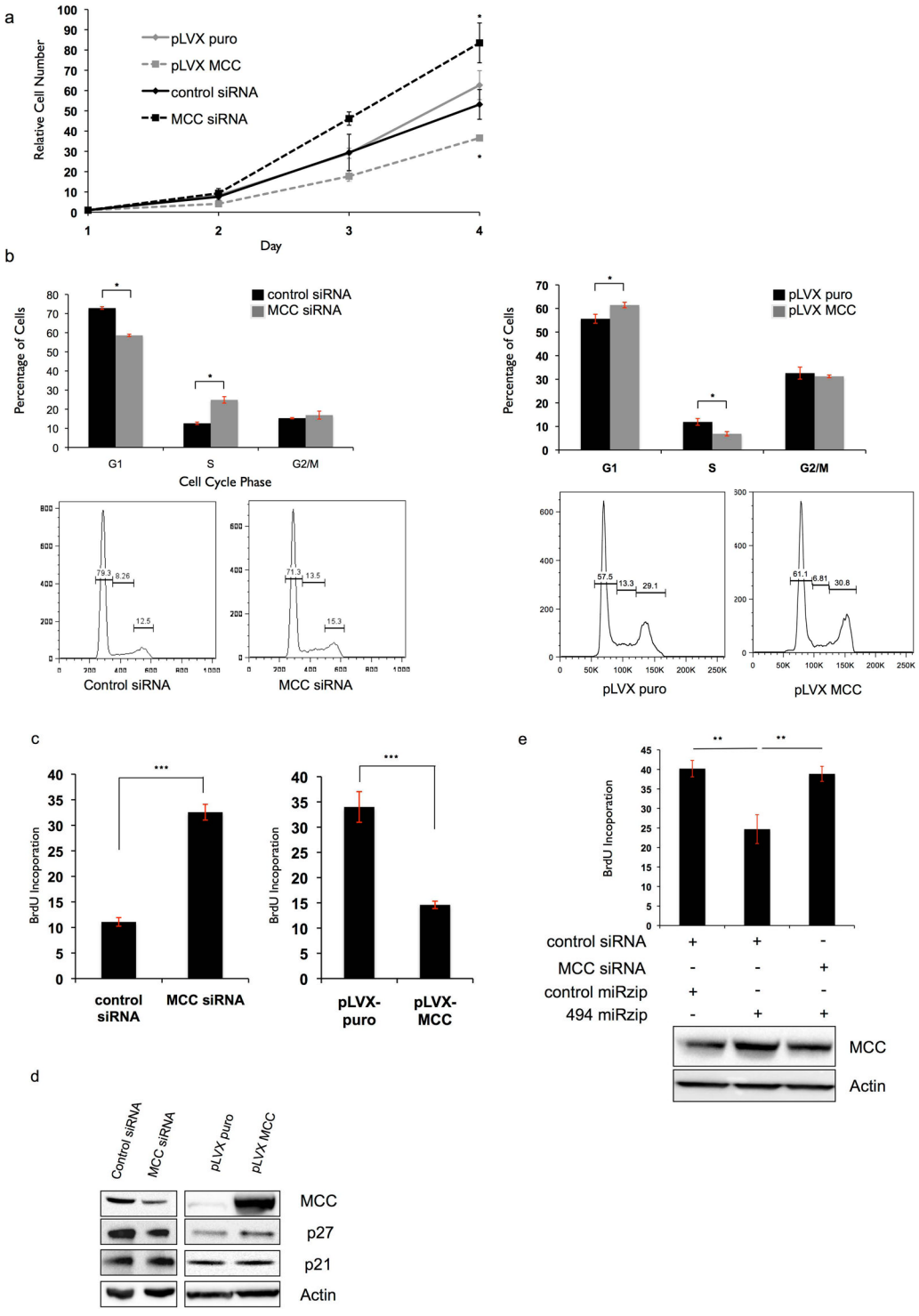

Figure 5. miR-494 modulates G1/S transition through suppression of MCC expression

A. LT2MR cells undergo increased proliferation with MCC inhibition and decreased proliferation with enforced MCC expression. Experiments were repeated 3 times and values are from 1 representative experiment. **B.** LT2MR cells exhibit accelerated G1/S transition with MCC inhibition and G1/S delay with MCC overexpression. LT2MR cells transfected

with control or MCC siRNA (top panel) and pLVX puro or pLVX MCC for 48 hours were stained with PI for FACS analysis. Cell cycle profiles were analyzed using FlowJo Analysis Software. Experiment was done with three replicates per sample and figure is representative of three experiments. **C.** Increased proliferation is due to accelerated G1/S transition in MCC siRNA transfected cells. LT2MR cells were transfected with either control or MCC siRNA (left panel) or pLVX puro or pLVX MCC (right panel) for 48h and exposed to BrdU for 40 min. Flow cytometry was used to measure BrdU incorporation. Experiment was repeated 3 times with 3 replicates per sample and values are from 1 representative experiment. ***$p<0.001$. **D.** Expression of cell cycle inhibitors corresponds to proliferation rate. LT2MR cells were transfected with either control or MCC siRNA (left panel) or pLVX puro or pLVX MCC (right panel) for 48h and tested for expression of p27 and p21 by western blot. **E.** Downregulation of MCC attenuates the effects of miR-494 inhibition on cell proliferaion. LT2MR cells were transfected with pmiRZip control or pmiRZip 494 and control or MCC siRNA as indicated and tested for MCC expression after 48h by western blot. Cell proliferation was assessed in these cells by measuring BrdU uptake over a period of 40 min. **$p<0.01$.

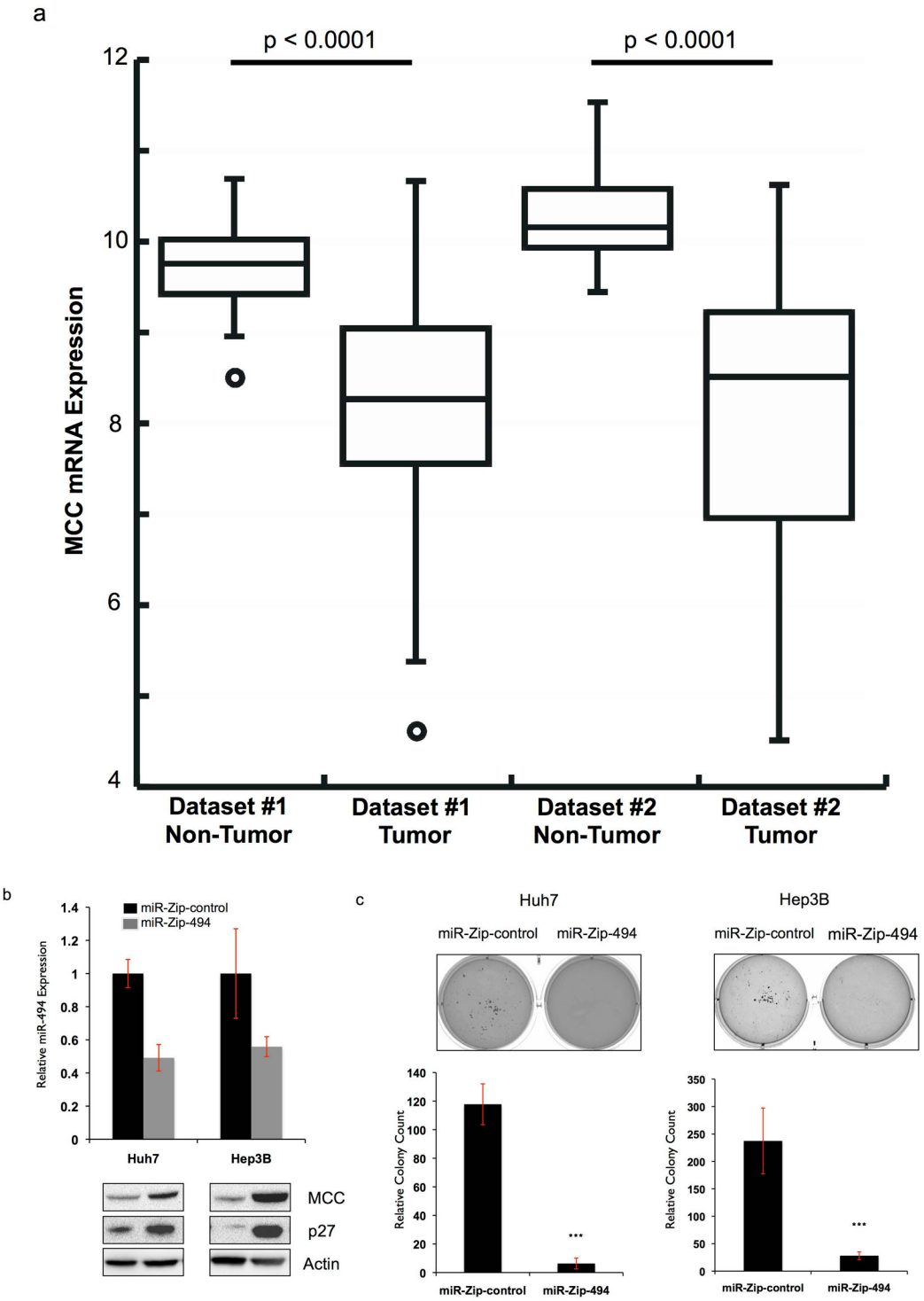

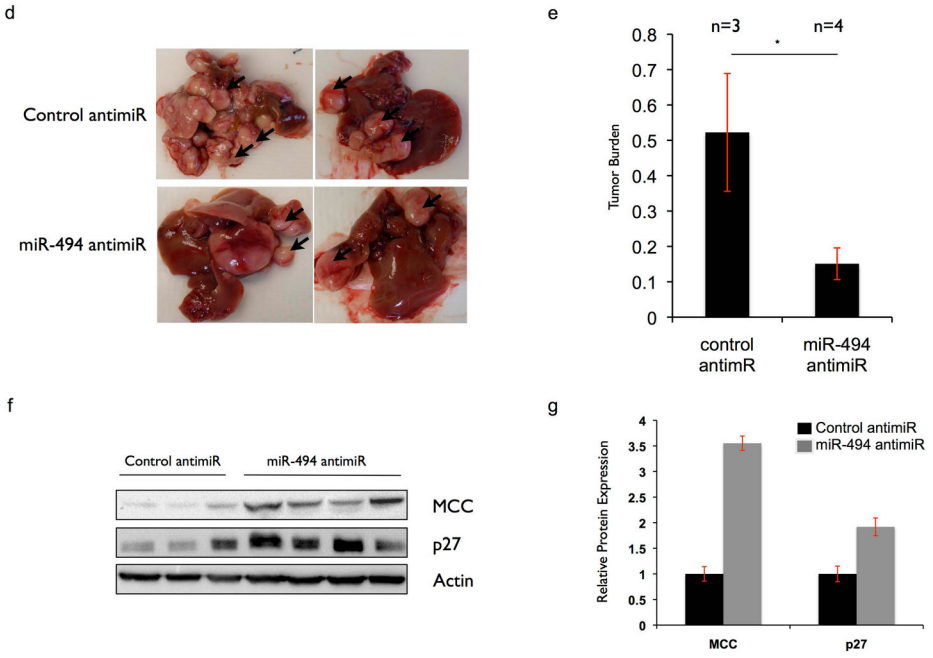

Figure 6. miR-494 inhibition decreases transformation in human and mouse HCC models

A. Decreased MCC mRNA expression in two human HCC datasets. MCC mRNA expression in tumor versus non-tumor tissues is shown for the Burchard (Dataset#1) and TCGA LIHC (Dataset#2). The bottom and top of the boxes indicate the first and third quartiles, the band inside the box is the median value. The whiskers represent the minimum and maximum values; the points indicate outliers. **B.** miR-494 knockdown increases MCC expression in Huh7 and Hep3B cells. miR-494 was stably knocked down in Huh7 and Hep3B cell lines with p-miR-ZIP-494. miR-494 expression was tested by qRT-PCR and calculated relative to p-miR-ZIP-control cell lines. MCC and p27 expression was tested by western blot. **C.** miR-494 inhibition decreases colony formation in Huh7 and Hep3B cells. Stable p-miR-ZIP control or 494 Huh7 and Hep3B cells were plated in soft agar for 2 weeks. Experiment was repeated three times in triplicate.***p<0.001 **D and E.** miR-494 inhibition decreases liver tumor growth *in vivo*. **D.** Representative pictures of livers of LT2/MYC mice (35) injected with control (n=3) or miR-494 (n=4) antimiRs over a period of 3 weeks (total 8 weeks off dox), twice a week. **E.** Relative tumor burden in mice as quantified by ImageJ. *p<0.05. **F and G.** miR-494 inhibition increases MCC and p27 expression *in vivo*. **F.** Protein expression of MCC and p27 in liver tumors of control and miR-494 antimiR injected mice. **G.** AntimiR-494 treated tumors show increased MCC and p27 protein expression. Protein expression values were quantified using Biorad Chemidoc software. MCC and p27 expression was normalized to actin and the average expression of each protein was calculated in each treatment group to generate the graph.